Accepted Manuscript

Title: Age of the source of the Jarrafa gravity and magnetic anomalies offshore Libya and its geodynamic implications

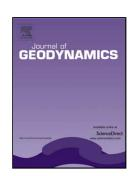
Authors: Giuma Reeh, Tahar Aïfa

PII: S0264-3707(08)00003-3 DOI: doi:10.1016/j.jog.2008.01.001

Reference: GEOD 830

To appear in: Journal of Geodynamics

Received date: 18-6-2007 Revised date: 31-12-2007 Accepted date: 1-1-2008



Please cite this article as: Reeh, G., Aïfa, T., Age of the source of the Jarrafa gravity and magnetic anomalies offshore Libya and its geodynamic implications, *Journal of Geodynamics* (2007), doi:10.1016/j.jog.2008.01.001

This is a PDF file of an unedited manuscript that has been accepted for publication. As a service to our customers we are providing this early version of the manuscript. The manuscript will undergo copyediting, typesetting, and review of the resulting proof before it is published in its final form. Please note that during the production process errors may be discovered which could affect the content, and all legal disclaimers that apply to the journal pertain.

Age of the source of the Jarrafa gravity and magnetic anomalies offshore Libya and its geodynamic implications

Giuma Reeh 1, Tahar Aïfa 2,*

¹Libyan Petroleum Institute, P.O.Box 6431, Tripoli, Libya ²Géosciences-Rennes, CNRS UMR6118, Université de Rennes 1, Campus de Beaulieu, 35042 Rennes cedex, France, *e-mail: tahar.aifa@univ-rennes1.fr

Abstract

The interpretation of the Jarrafa magnetic and gravity highs, NW Libyan offshore, suggests that it may be caused by a body of high density and high magnetization. Analysis of their power spectra indicates two groups of sources at: 1) 2.7 km depth, probably related to the igneous rocks, some of which were penetrated in the JA-1 borehole, 2) 5 km depth, corresponding to the top of the causative body and 3) 10 km depth, probably referring to the local basement depth. The boundary analysis derived from applied horizontal gradient to both gravity and magnetic data reveals lineaments many of which can be related to geological structures (grabens, horsts, faults).

The poor correlation between pseudogravity fields for induced magnetization and observed gravity fields strongly suggests that the causative structure has a remanent magnetization (D=- 16° , I= 23°) of Early Cretaceous age, fitting with the opening of the Neo Tethys 3 Ocean.

Three-dimensional interpretation techniques indicate that the magnetic source of the Jarrafa magnetic anomaly has a magnetization intensity of 0.46 A/m, which is required to simulate the amplitude of the observed magnetic anomaly. The magnetic model shows that it has a base level at 15 km.

The history of the area combined with the analysis and interpretation of the gravity and magnetic data suggests that : 1) the source of the Jarrafa anomaly is a mafic igneous rock and it may have formed during an Early Cretaceous extensional phase, 2) the Jarrafa basin was left-laterally sheared along the WNW Hercynian North Graben Fault Zone, during its reactivation in the Early Cretaceous.

Keywords: Jarrafa, Gravity, Magnetics, Early Cretaceous extension, igneous rocks

1- Introduction

The study area is located between [12° 51'E - 13° 57'E] and [33° 50'N - 34° 43'N] (Figure 1). The Jarrafa magnetic and gravity anomalies lie in a region known as Pelagia, which is a salient of the African plate and represents an unstable continental margin formed during the Carboniferous collision of the African and the Apulian plates. This region has experienced a number of major tectonic events, namely Hercynian compression, Jurassic extension and Alpine Orogenic compression (Dewey et al., 1989). During the Hercynian event the area was extensively restructured, forming the strong WNW fault system that has subsequently dominated its structural evolution.

The magnetic and gravity data used in this study were obtained from shipborne measurements by various contractors in the period 1975-1987; they have been collated by the National Oil Corporation of Libya. The anomalies considered in this study were identified from magnetic and gravity data prepared by the Simon-Robertson Company for Sirt Oil Company.

The distribution of the gravity and magnetic measurement points along profiles within the study area are shown in Figure 2. There are 166571 magnetic and 180955 gravity points. The latter were fully corrected for topographic effects using a reduction density of 2.2 cgs. Densities and magnetic susceptibilities of sedimentary basin and crystalline basement rocks are desirable for any magnetic and gravity data interpretation. Unfortunately, neither density nor magnetic susceptibility measurements are available for the rocks of the study area.

The Jarrafa magnetic and gravity anomaly maps (Figures 3a-b) were gridded with a 2 km grid cell size and mapped at 1 mGal contour intervals for gravity and 20 nT for magnetics. The magnetic data show that the magnetic anomaly has an amplitude of 200 nT, and a small low in its northern part, indicating a magnetization dipping steeply to the north.

The gravity anomaly has a maximum value of 24 mGal with values dropping down to their lowest levels towards the SW. The gravity anomaly trends WNW and the Jarrafa-1 borehole is located at its northwest end. It is probably related to the north Graben fault zone (NGFZ) as shown on the tectonic map.

Jongsma et al. (1985) have interpreted the long wavelength of magnetic anomalies in the NW Libyan offshore as being caused by the presence of Jurassic and Late Cretaceous volcanics. The regional background of the magnetic map of NW

offshore Libya has been defined as a weak magnetic basement overlain by a thick sequence of non-magnetic sediments (Dewey et al., 1989), while the strong anomalies are probably intrusive volcanic plugs which penetrate the overlying sediments.

The aims of the present study are to interpret the anomaly in terms of three-dimensional models. Its purpose is to define the relation between the gravity and magnetic lineament and geological structures by means of geophysical methods. We can expect the geophysical data to illuminate the deep geology, which is complicated by the above mentioned orogenic phases, and to help understand the structural development of the Jarrafa basin and its geodynamic implications.

2- Geology

There are several wells in the Libyan offshore area that penetrated igneous rocks, some of them on more than one horizon. Most of these wells show that volcanics become more common towards the boundary between continental and oceanic crust (NE of the study area; Seddig, 1992). The thickest and most significant volcanics in the Libyan offshore area occur in the Jarrafa-1 borehole (Figure 4) which penetrated thick volcanic rocks. In the Upper Cretaceous 434 m of basalts and volcanic breccias were reported at a depth of 2467 m, emplaced in the Turonian-Cenomanian interval. The Lower Cretaceous contains 100 m of basalts emplaced in the Albian-Aptian interval. The borehole was drilled near the centre of the anomaly but was apparently not deep enough (3373 m) to reach the source of the gravity and magnetic anomalies, the top of which is estimated at almost 5 km.

a) Tectonic setting

The Pelagian block is a collective term for the area to the north of the Libyan Coastal Fault system, which separates it from the relatively stable Saharan platform to the south. The Pelagian block, which is underlain by continental crust, is a part of the African plate that abuts the Apulian plate to form a continental block separating the Eastern and western Mediterranean Ocean basins.

Since the Hercynian there has been a more or less continuous relative motion between the African and European plates, which did not actually separate them until the middle Jurassic. This motion was complex with several changes in direction (from NW-SE convergence prior to the Late Miocene to roughly N-S or NNW-SSE convergence) resulting in complicated structures with repeated reactivation (Ziegler,

1992). Global plate models suggest NNW convergence of the African and European Plates in the Mediterranean north of Libya (Livermore and Smith, 1985). The geological history of Pelagia has been described by a number of different authors (e.g. Dewey et. al., 1973; Biju-Duval et. al., 1977; Pitman et. al., 1981; Finetti, 1982; 1984; 1985; Dewey et al., 1989; Pavoni, 1993). The tectonic history of the study area, since the Late Carboniferous, has been divided into four periods that correspond to large scale plate tectonic episodes: the Hercynian event extends from the Late Carboniferous into Late Permian; the stabilization of the Pangea supercontinent, after its assembly during the Hercynian, from Late Permian to middle Triassic; the initial break-up of Pangea, beginning with Late Triassic rifting, that culminated in the opening of the Central Atlantic and Neo-Tethys Oceans in the Middle Jurassic, and continued to the mid-Cenomanian (Late Triassic to mid Cenomanian); and the Alpine Orogeny, driven by the convergence of Africa and Europe, starting in the mid-Cenomanian and continuing to the Present. Within this broad framework, Dewey et. al. (1989) recognized nine distinct tectonic phases, each associated with a change in relative plate motions and the resulting reorientation of the stress field over Pelagia. A brief discussion of these phases follows:

- 1. Late Carboniferous to Late Permian: During the Hercynian event Gondwanaland and Laurasia collided to form the supercontinent of Pangea. Although Pelagia lay outside the orogenic belt that developed along the collisional suture, its basement was restructured by a series of major WNW trending faults. These faults developed as part of major right-lateral shear zones that extended across southern Europe and Northern Africa. Within Pelagia the most important of these Hercynian faults were the Jeffara fault, the Libyan Coastal fault system, the South Graben fault zone (SGFZ), the NGFZ and the Melita Graben fault zones. In the later stages of this event, right-lateral motion along the Libyan coastal fault system and the SGFZ caused compression and fault uplift in the area that was to become the Sabrata basin.
- 2. Late Permian to Middle Triassic: After the Hercynian event there was a short period, corresponding to this phase, when the continent of Pangea was fairly stable. With this stability the strike-slip motion of the Hercynian fault system ceased. In Pelagia this was a tectonically quiet period with no major structural events.
- 3. *Late Triassic to Middle Jurassic:* This phase corresponds to the initial breakup of Pangea, when rifting started between Africa and North America along a zone which was to become the central Atlantic Ocean. Different rates of extension along this zone

resulted in the separation of Africa and Europe. Africa was moved left laterally with respect to Europe. According to this motion the WNW Hercynian faults were reactivated and moved left laterally. This left lateral motion caused the initiation of the Sabratah basin as a pull-apart between the Libyan Coastal fault system and SGFZ.

- 4. *Middle Jurassic to Middle Cenomanian:* After the opening of the central Atlantic, Africa drifted away from Europe to the SE, the boundary between the plates began to fragment and the Apulian and Anatolian microplates drifted away from North Africa, opening the Neo-Tethys 3 Ocean. Northern Pelagia became a passive margin of this new ocean and began to subside thermally.
- 5. *Middle Cenomanian to Maastrichtian:* In this phase the motion of Africa relative to Europe changed from southward divergence to northeastward convergence. This event is usually regarded as marking the onset of the Alpine Orogeny and corresponds with the beginning of this phase.
- 6. *End of Cretaceous to Ypresian:* During this phase there was no detectable relative motion between the African and European plates. The Jarrafa basin, which lies along the northern side of the NGFZ, began to subside at this time.
- 7. End of Ypresian to end of Eocene: During this phase the motion of the African plate with respect to the European plate had a NNE direction. In both the Sabratah and Jarrafa basins there was an increase in subsidence.
- 8. *End Eocene to Tortonian:* During this phase, and until the middle of Burdigalian, Africa had northward convergence with respect to Europe. From the middle of Burdigalian until the end of the Miocene the direction of convergence changed to NNE.
- 9. *Messinian to Recent*: During this phase, the motion of Africa relative to Europe changed from NNE to NW. The effect of this change in plate motion was the reactivation of WNW Hercynian fault zones, which produced a number of deep grabens across Pelagia. These include the south, north Graben fault zones in the Libyan offshore.

b) Igneous activity

The volcanism in the central part of the Mediterranean area has been investigated by many authors (e.g Zarudski, 1972; Di Paola, 1973; Finetti, 1982: Jungsma et al., 1985). Throughout the Pelagian Shelf, volcanic activity has been intermittent from Triassic to Quaternary with strong local activity in the Jurassic,

Cretaceous and middle Late Miocene to Quaternary. Igneous rocks occur as intrusive dikes, laccoliths and extrusives. Finetti (1982) divided the history of the central Mediterranean into four extensional phases on the grounds of numerous available geological, geophysical and well data: 1- Middle to Upper Triassic, 2- Middle Jurassic, 3- Upper Cretaceous, 4- Neogene-Quaternary.

The first extensional phase started in the middle Triassic and continued through the Late Triassic. Many basaltic horizons have been found in wells in the Ragusa-Malta area as evidence of this large movement.

The second extensional phase occurred in the middle Jurassic, when the most impressive and prominent volcanic activity of the Sicily-Malta area took place. Practically, over a large part of this province, this stratigraphic interval is completely or almost completely made up of igneous rocks. In Malta and along the Sicily-Malta escarpment middle Jurassic volcanic rocks are found.

The third extensional phase occurred during the Late Cretaceous. In the Sabratah basin there is evidence of extensional tectonics with faulting and basaltic effusions widely distributed at this time.

The last extensional phase occurred during the Neogene-Quaternary. During this phase faulting activity affected the whole Pelagian Sea. This rifting phase is associated with prominent volcanic activity in many zones of the Pelagian and Ionian Seas. Impressive volcanic bodies are recognized in the Ionian abyssal basin, the most important one being the Marconi seamount area where the thinnest crust conditions of the Ionian Sea exist and the maximum Bouguer gravity anomaly of the Mediterranean area is found (310.0 mGal) (Finetti and Morelli, 1973).

The Sicily Channel has the typical tectonic structure of a continental rift valley formed by three main graben trending NW-SE (Pantelleria, Malta and Linosa Graben). Geophysical studies (Allan and Morelli, 1971) show that an up to 90.0 mGal positive Bouguer anomaly exists along the axes of all three graben which affect this part of the Mediterranean Sea. Positive magnetic anomalies occur near Pantelleria, Linosa and in other areas of the Sicily channel (Zarudski, 1972). The magmatic activity in the Sicily Channel has been relevant since the early Quaternary up to Recent. The volcanism is strictly related to the particular tectonic structure of this area. The main feeding fractures of the volcanism in Pantelleria and in Linosa, together with the elongated shapes of submerged volcanic relief, are parallel to the main tectonic trend (NW-SE) of the Sicily Channel rift valley. Barberi et al (1969)

obtained a K/Ar age for the Linosa rocks of less than 1 Ma. All the rocks from Pantellena and Linosa have basaltic affinities (Di Paola, 1973).

A brief comparison of the four extensional phases introduced by Finetti (1982) with the nine extensional and compressional phases proposed by Dewey et al. (1989) shows that both authors have agreed to call the Jurassic and Triassic phases extensional phases, but there is a conflict between the Late Cretaceous and Neogene-Quaternary phases: Finetti (1982) calls them extensional phases based on the volcanic rocks that were found in the boreholes and traced in the seismic profiles, while Dewey et al. (1989) stated that, since the Late Cretaceous, there has been compression between Africa and Europe based on the study of their relative motion. It seems the classification of nine phases produced by Dewey et al. (1989) is more accurate than that produced by Finetti (1982).

However, Ziegler (1992) stated that the Italo-Dinarid block split from Africa during the Late Jurassic. Dewey et al. (1989) indicated that, during the Middle Jurassic, the Apulian and Anatolian plates pulled away from North Africa, opening the Neo-Tethys 3 Ocean between Africa and Europe. Thus the Libyan continental edge was converted into a passive rift margin (Dewey et al. 1989). At other passive margins continental volcanism is often widespread during rupture (White, 1987). Thus, the igneous rocks encountered in the boreholes in the NW Libyan offshore are probably related to the reactivation of Hercynian basement faults due to the change of the stress field direction between the African and European plates, allowing magma to erupt as lava flows. During the same period plutons, emplaced in the Jurassic and Triassic in the Libyan offshore and near the Ragusa-Malta area, were probably related to extension during Jurassic-early Cretaceous times. This area is the edge of the African continent where the Apulian and Anatolian Plates pulled away in the mid-Jurassic, forming the Neo-Tethys 3 Ocean in their wake. Considerable volcanic activity would be expected in such a passive margin setting.

3- Geophysical data

a) Power spectrum analysis

From the digital data used to prepare Figures 3a and 3b, the azimuthally-averaged power spectra were computed for both the magnetic and the gravity anomalies. Spector and Grant (1970) showed that for an ensemble of prismatic blocks with infinite depth extent the logarithmic radial energy spectrum of the total magnetic

intensity consists of a straight line whose gradient is related to the average depth to the tops of the prisms. Furthermore, in the case of a double ensemble of prisms, two gradients would normally be obvious in the spectrum, with the steep gradient related to the deeper sources and the low gradient related to the shallow sources.

Figure 5a shows the graph of azimuthally-averaged power spectrum against wave number for the magnetic data. Three linear segments are apparent before significance is lost in digitization noise, indicating the presence of three discrete magnetic sources at different depths. The statistical model of Spector and Grant (1970) allowed source depth estimates to be derived from the slopes of these segments. For the magnetic anomalies these were computed at 2.7 km, 5.0 km and 11.0 km below sea level. The gravity spectra shows that it arises from four sources at different depths computed at 2.3 km, 5.0 km, 9.4 km and 13 km. The deepest gravity source is probably related to the base of the Jarrafa causative body, the other sources are similar to the magnetic sources (Figure 5b). In addition, a power spectrum of the reduced to the pole magnetic grid, which represents the magnitude of the various frequency components of a 2D image that has been Fourier transformed, has been computed and seems in agreement with the location of the main source at the origin of the anomaly. The shallow source is probably related to the volcanic rock encountered in the borehole, the intermediate source represents the causative body underlying the Jarrafa anomaly, and the deeper source may represent the depth to the local basement. The nature of the basement in the Libyan offshore is still unknown. In fact, the deepest well in the Libyan offshore (L1-137) was drilled in the Sabratah basin, reaching the Upper Triassic succession, but it is generally accepted that most of the Palaeozoic was eroded during the Hercynian orogeny and the Triassic sediments are thought to be unconformably lying on a Precambrian basement. (Dewey et al., 1989).

b) Magnetic and Gravity interpretation

The magnetic anomaly map is more difficult to interpret than the gravity map. This is because of the shifting of the magnetic anomaly away from the apex of the underlying source by the inclination of the present day field. Additionally, the remanent magnetization associated with any magnetic body may cause further complications.

In order to compensate for this shift, the pseudogravity anomaly (Baranov, 1957) is produced from the magnetic anomaly using the induced magnetization

direction and keeping the ratio of intensity of magnetization to density at unity. The pseudogravity is used for magnetic interpretation to determine the edges of source body. Furthermore, the comparison of pseudogravity with observed gravity is made to see if the same feature is generating both gravity and magnetic anomalies.

We used in our calculations the transform of the Poisson equation relating the gravity and magnetic field potentials expressed by $U = -\frac{J}{G\rho} \frac{\partial V}{\partial I}$, where U, V, I, J, ρ , G respectively, magnetic potential, gravitational potential, direction of are, magnetization, magnetization intensity, density and Gravitational constant. The application of this transform is well known and has been applied successfully (Bilim and Ates, 1999, 2004). The pseudogravity field of the Jarrafa magnetic anomaly for induced magnetization of the present day field (D= 0°, I=47°) shows poor correlation with the observed gravity field (Figure 6a), suggesting that the causative body has a remanent magnetization. Consequently several different magnetization directions were used in the pseudogravity transformation and it was found that (D=-16°, I=23°) provided a pseudogravity field in which the maximum anomaly is correlated with the maximum observed gravity (minimization) (Figure 6b). The orientation of the magnetization appears to be the most realistic estimate of the total magnetization vector orientation. Using the master apparent polar wander path for Africa (Besse and Courtillot, 1991), and reducing the data to the Jarrafa basin (34°N, 13°E), we notice that this direction of magnetization is Early Cretaceous in age. This age, which ranges between 160 and 170 Ma, fits with the opening period of the Neo Tethys ocean. At this time, the SE oriented stress direction (phase 4) mentioned by Dewey et al. (1989) accommodates the extensional opening of the main structural features. As an example, the orientation of most all of the Graben faults, graben elongations, and the Jarrafa basin are parallel to this stress direction. We also notice that the south-eastern part of the Jarrafa basin is rotated counter-clockwise according to the gravity map (Figure 3b).

The pseudogravity field for the induced magnetization direction was interpreted using the iterative method of Cordell and Henderson (1968), in which the pseudogravity anomaly is simulated by that produced by a suite of vertical rectangular prisms, one per datum point. The prisms were assumed to have a common base level. Each prism has a horizontal cross-section of 2 km x 2 km. Several runs of the routine with different base levels were necessary so that the body reached the minimum depth

of 5 km suggested by power spectrum analysis; the base level was then 15 km. The model is shown in Figure 7a in terms of contours on the centres of the top of each prism.

The magnetic anomaly (Figure 3a) of the model was then calculated using a 3-D Fortran code (see Kearey, 1991). The calculated magnetic anomaly was adjusted to simulate the amplitude of the observed magnetic anomaly (Figure 7b). The adjustment factor indicates 0.46 A/m to be the total intensity of magnetization. Comparison of both observed magnetic anomaly (Figure 3a) and the calculated magnetic anomaly (Figure 7b) shows that the magnetic anomaly of the model is similar to the observed field.

The gravity field (Figure 3b) over the same area as the magnetic field appears to show a positive anomaly with a maximum value of 24 mGal associated with the magnetic anomaly. It is flanked to the NE by the WNW trending negative anomaly of the Jarrafa basin and to the SW by the same WNW trending negative anomaly of the Sabratah basin. Since the density and density contrast of the causative body are the fundamental factors controlling the gravity anomaly, reliable density values are required for the gravity modelling. Unfortunately, the Jarrafa-1 borehole did not penetrate the body which caused the anomalous gravity and magnetic fields and, therefore, no rock sample was available for measuring the physical properties of this body.

The assumption was made that the source body has the same composition as the shallow igneous rocks that were penetrated by the Jarrafa-1 borehole at 3373 m. The shallow igneous rocks there have a basaltic composition (Figure 4) and have a density in the range 2.70-2.90 cgs, whereas the density of the upper crust is 2.68 cgs. A density contrast of 0.12 cgs was consequently adopted for this body. This appears to be the most realistic estimate of the density contrast value for the causative body.

The gravity anomaly was interpreted using a 3-D gravity anomaly technique (Cordell and Henderson, 1968), using the same Fortran code as before (Kearey, 1991). Different base levels were tried until the top of the model was 5 km as calculated from the power spectrum (Figure 5b), the appropriate level being 13 km (Figure 8a). The gravity anomaly of the model was then calculated (Figure 8b). Comparison of the calculated and the observed gravity anomalies shows a reasonable fit.

In terms of magnetic and gravity boundary analysis, Cordell and Grauch (1982, 1985) presented a technique to estimate the location of abrupt changes in magnetization or density of upper crustal rocks. The method first requires transformation of the magnetic anomaly into the pseudogravity anomaly, which is the gravity anomaly that the magnetized body would produce if it was of uniform magnetization and density; the next step is to calculate the magnitude of the horizontal gradient of the pseudogravity anomaly and to plot the location of their maxima, which approximately overlie the edges of the body. Blakely and Simpson (1986) extended this procedure to accelerate and automate the final step by comparing each grid intersection with its eight nearest neighbours in four directions along the row, column and both diagonals to see if a maximum is present. Maxima are displayed at four significance levels (N). The counter N is increased by one for each satisfied inequality, ranging from 0 to 4 and provides a measure of the quality of the maximum. Their method was applied to the magnetic and gravity data of the Jarrafa anomaly.

The magnetic field was transformed into a pseudogravity field using a 23° inclination and -16° declination. From the pseudogravity field the magnitude of the horizontal gradient was calculated. Then by comparing each grid intersection with its nearest neighbours in four directions using N=2: east to west, north to south and along both diagonals, the maximum was obtained. The pattern of maxima in the horizontal gradients provides the outline of the Jarrafa, magnetic body (Figure 9a).

The horizontal gradient of the gravity field, from which the maxima of the horizontal gradient are calculated with N=3 are plotted as crosses on the map (Figure 9b). The sinuous traces of maxima represent the major horizontal gradients of the gravity field. Many of these gradients can be attributed to geological bodies and major structures. The map (Figure 9b) is rather more complex than for the magnetic field because of the more numerous gravity anomaly sources arising from density contrasts within both sediments and basement.

The depth estimates to the magnetic sources were obtained using Euler deconvolution as described in the following equation (Reid et al., 1990):

$$(x-x_0).\frac{\partial M}{\partial x}+(y-y_0).\frac{\partial M}{\partial y}+(z-z_0).\frac{\partial M}{\partial z}=N.(B-M)$$

where, (x_o, y_o, z_o) is the position of the magnetic source whose total magnetic field M is measured at (x,y,z). The total magnetic field has a regional value of B and N is the

structural index which is equal to three for a point dipole and two for a vertical pipe. More complicated bodies have indices ranging from zero to three. The technique is based on the concept that the magnetic fields of localized structures are homogeneous functions of the source coordinates and therefore satisfy Euler's equation.

Euler deconvolution provides a powerful tool to facilitate the mapping of geological contacts and faults. It was performed on the reduced to pole total magnetic field grid using a structural index of zero (suitable to map geological contacts) with a window size of 12km. The structural index is a measure of the rate of change with distance of the total magnetic field. The various structural indices (SI) for simple models in a magnetic field are: (a) 0.0 for geological contacts and faults, (b) 0.5 for thick step, (c) 1.0 for sills and dykes, (d) 2.0 for pipes, and (e) 3.0 for spheres.

The Euler deconvolution solutions for depths ranging from 2km to 10 km are plotted in Figure 10 on a contoured image of reduced to pole total magnetic field. They are plotted as a series of colour circles, with the colour of each indicating the depth to magnetic source and the centres indicating the position of the source. Since we used a structural index of 0.0 to calculate the Euler solutions, we expect that the map shows the position and depth of faults and geological contacts formed as a result of juxtaposed rocks of various magnetic compositions. However, the NGFZ is probably not a magnetized fault.

A composite map constructed from combining the results of the gravity and magnetic interpretations is displayed in Figure 11. The map is self-explanatory and shows that the main tectonic features in the area are oriented in a NW-SE direction in agreement with the mapped tectonic elements. This map shows major trends (Figure 11): the boundary of the causative body of the Jarrafa anomaly, Jarrafa basin, and the Sabratah basin North and South Grabens fault zone is defined.

4- Discussion and conclusions

The causative body of the Jarrafa anomaly is deeper than that of the igneous rocks penetrated in the Jarrafa-1 borehole, suggesting that these igneous rocks do not contribute significantly to the gravity and magnetic anomalies because of either their low density and magnetization or their alteration.

The high amplitudes of the gravity and magnetic anomalies indicate that they are caused by a high-density, magnetized igneous body that probably comprises mafic igneous rocks, as these are the most common lithologies with these properties. According to the lithologies of rocks found in the Jarrafa-1 borehole, the volcanics, which are composed mainly of breccias and basalts, occur at two different depths, shallow at 2467 m and intermediate at 3272 m. It seems that there is a correlation between the power spectra depths for the shallow source (2.3 km for gravity and 2.7 km for magnetics, Figure 5) and the shallow depth from the borehole (~2.5 km). The Jarrafa source body, which is located in the horst area between the SGFZ and the NGFZ, is elongated in a NW-SE direction. It shows two maxima with two different depths (5 km, 6 km) suggesting a dipping direction to the southeast. During the Late Carboniferous, the NGFZ developed as a partly lateral mega-shear zone (Dewey et al., 1989). The north-eastern part of the body is controlled tectonically by the NGFZ, which is steeply dipping to the northeast. According to the gravity and magnetic fields, the Jarrafa basin was left-laterally sheared along the NGFZ (Figure 11) during its reactivation. The age of this reactivation is correlated with the emplacement of the Jarrafa source body, which is deduced from the magnetization age given by the master apparent polar wander path at Early Cretaceous times. It is in agreement with the reactivation of the WNW Hercynian faults, which moved left-laterally in the period ranging from Late Triassic through middle Cenomanian (Ziegler, 1992).

By comparing both magnetic (Figure 3a) and gravity (Figure 3b) maps one can respectively see a single anomaly and two local anomalies with varying amplitudes. The 3D magnetic model shows two highs (Figure 7a), caused by magnetized bodies located at 5 km and at 6 km, in agreement with the gravity highs shown in the 3D gravity model (Figure 8a). This suggests that both the gravity and magnetic anomalies are caused by the same igneous body. The calculated gravity anomaly using a density contrast of 0.12 cgs is probably affected by a structural relief above the igneous body.

There are several wells in the Libyan offshore area that penetrate igneous rocks, some of them at more than one horizon as shown in Figure 4. Most of these

wells show that volcanics become more common towards the boundary between continental and oceanic crust (northeast of the study area; Seddig, 1992). The thickest and most significant volcanics, consisting of basalts, in the Libyan offshore area occur in the Jarrafa-1 well which penetrated predominantly volcanics of 434 m thickness in the Turonian-Cenomanian. It also penetrated 100 m volcanics in the Albian-Aptian. An unconformity suggests some evidence that the uppermost volcanics were emplaced during a tectonic event, probably the southeast extensional regime related to the southeast drift of Africa during Early Cretaceous times.

Livermore and Smith (1985) and Ziegler (1992) indicated that the rapid opening of the central Atlantic Ocean in the Late Jurassic - Early Cretaceous was accompanied by an 8° clockwise rotation of Laurasia and major sinistral translations between Africa and Europe. Jongsma et al. (1985) indicated that the Early Jurassic volcanics within the Jurassic section are related to break-up at about 180 Ma. Dewey et al. (1989) indicated that, during the Middle Jurassic, the Apulian and Anatolian plates pulled away from North Africa, opening the Neo-Tethys 3 ocean between Africa and Europe. Thus, the Libyan continental edge was converted into a passive rift margin. At other passive margins continental volcanism can be widespread during such rupture (White, 1987). For example, when the northern north Atlantic opened during the Tertiary, the igneous province produced in Britain, Northern Ireland and Greenland is thought to be related to the rifting and the thermal anomaly produced by a mantle plume. This plume is still active and it may be responsible for the active volcanoes of Iceland (White and Mckenzie, 1989). Furthermore, rifting during the Mesozoic opened a series of sedimentary basins in northwest Europe, such as the More and Voring basins off Norway and the Rockall Trough off northwest Britain and Ireland (White and Mckenzie, 1989). In the Libyan offshore there is no evidence to show that the central Mediterranean was underlain by a hotspot during the Mesozoic. Rather, a rift opened basins in the Libyan offshore (including, for example, the Sabratah basin). This margin apparently did not develop into a true volcanic margin like those in the northern north Atlantic. Thus, the causative body of the Jarrafa anomaly was probably intruded into the upper crust as a result of extensional forces acting during the Jurassic-Early Cretaceous.

Based on the tectonic history of the area, apart from the Jurassic-Early Cretaceous extensional phase, there is no other tectonic mechanism that can produce such a large amount of magma. Although no attempt has been made to date the

igneous rocks encountered in the Jarrafa-1 borehole, they were probably intruded into the upper crust during the Cretaceous. North of the NGFZ (Figure 11), there is no significant gravity or magnetic signature (Figures 3a, 3b).

According to our understanding of the opening of the Central Atlantic Magmatic Province (CAMP), we may suggest that, as recorded eastward in the Reggane basin (Smith et al., 2006), the far-field-stress effect related to either the Cimmerian phase (~140 Ma) or the Austrian phase (~125 Ma) could also be related to the small rotation mentioned by Ziegler (1992). The signature of this rotation was probably recorded in the south-eastern part of the Jarrafa basin as suggested by its counter-clockwise curvature. The mechanism of this counter-clockwise rotation could be accommodated by the left-lateral movement mentioned above.

The gravity and magnetic anomalies show a WNW trend; many tectonic elements in the Libyan offshore follow this trend, such as the Libyan coastal fault system, north and south Graben fault zones, Sabratah and Jarrafa basins. This trend is thought to have formed during Hercynian events resulting from the collision of Laurasia and Gondwanaland to form the Pangea supercontinent (Badham, 1982). The trend of the anomaly probably corresponds to pre-existing weaknesses in the continental lithosphere reactivated under extensional forces during Jurassic-Early Cretaceous times (see, for example, Courtillot, 1982). However, there is no evidence of the existence of such a trend in the Pre-Hercynian geological history of North Africa.

It is important to mention that the heat associated with intrusion into an organic-rich sedimentary rock may cause thermal alteration of the organic matter. Maturation of the organic matter in the vicinity of the intrusion can lead to the generation of liquid hydrocarbons. Many accounts record hydrocarbons at the margins of and in the vesicles of sills and dykes (e.g Parnell, 1985). Similarly the heat of an igneous pluton intruded into a suitable source rock could generate very substantial volumes of hydrocarbons. Calculations by Winkler (1979) suggest that the country rock around a 10 km wide granite intruded at 800°C and 1.2 km depth would remain at nearly maximum temperature for a million years. Therefore, the particular occurrence of hydrocarbons around the igneous rocks in the Libyan offshore could be related to the role of these igneous rocks as a thermal and/or structural focus. This idea still needs strong evidence for greater maturity of rocks from boreholes surrounding the igneous rocks.

Acknowledgements

We thank the National Oil Corporation of Libya and the Libyan Petroleum Institute for their permission to publish the present data. G.R. would like to thank them for the financial support and for a visiting Grant at Géosciences-Rennes (France). We are grateful to two anonymous referees who did some pertinent remarks allowing to improve this manuscript. Thanks also to Dr A.B. Reid for his advise concerning the application of Euler deconvolution.

References

- Allan T.D., Morelli, C., 1971. Geophysical study of the Mediterranean Sea. *Boll. Geofisica ed Applicata*, XIII, No.50, p.100-142.
- Badham J.P.N., 1982. strike-slip Orogens-an explanation for the Hercynides. *Journal* of the Geological Society of London, v.139, p.493-504.
- Baranov V., 1957. A new method for interpretation of aeromagnetic maps: Pseudogravity anomalies. *Geophysics*, vol.22 p.359-383.
- Barberi F., Borsi S., Ferrara G., Innocennti F. 1969. Strontium isotopic composition of some recent basic vulcanite of the southern Tyrrhenian Sea and Sicily channel. *Contr. Mineral. Petrol.*, Vol.23, p.157-172.
- Besse J., Courtillot V., 1991. Revised and synthetic apparent polar wander paths of the African, Eurasian, North American and Indian plates, and true polar wander since 200 Ma. *J. Geophys. Res.*, 96, B3, 4029-4050.
- Biju-Duval B., Dercourt, J., Le Pichon, X., 1977. from the Tethys Ocean to the Mediterranean seas: A plate tectonic model of the evolution of the western Alpine system. In: Biju-Duval, B. and Montadert L. (Eds), Structural history of the Mediterranean Basins, Paris, *Editions Technip*, p.143-164.
- Bilim F., Ates A., 1999. A computer program to estimate the source body magnetization direction from magnetic and gravity anomalies. *Computers and Geosciences*, V. 25, p. 231-240.
- Bilim F., Ates A., 2004. An enhanced method for estimation of body magnetization direction from pseudogravity and gravity data. *Computers and Geosciences*, V. 30, p. 161–171
- Bishop W.F, 1975. Geology of Tunisia and adjacent parts of Algeria and Libya. *American Association of petroleum Geologists Bulletin*, V.59, n°3, p. 413-450.
- Blakely R.J., Simpson R.W., 1986. Approximating edges of source bodies from magnetic or gravity anomalies. *Geophysics*, v.51, n°7, p.1494-1498

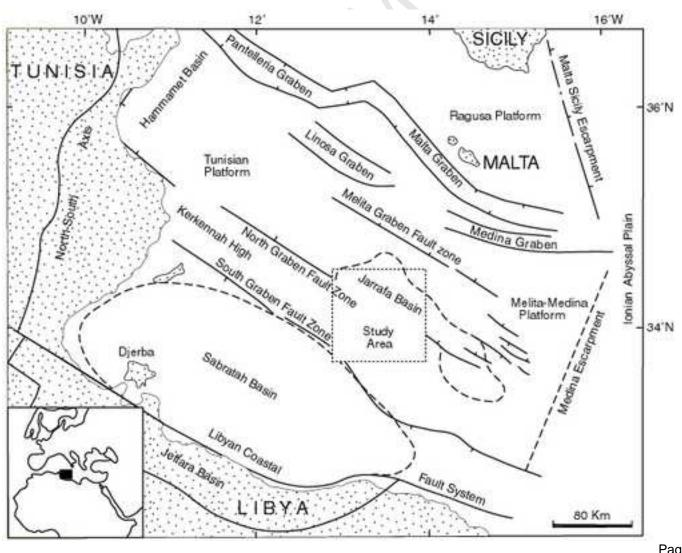
- Cordell L., Henderson R.G., 1968, Iterative Three-Dimensional solution of gravity anomaly Data using a Digital Computer. *Geophysics*, v. 33, p.596-601
- Cordell L., Grauch V.J.S., 1982. Reconciliation of the discrete and integral Fourier transforms. *Geophysics*, v. 47, n°2, p.237-243.
- Cordell L., Grauch V.J.S., 1985. Mapping basement magnetization zones from aeromagnetic data in the San Juan Basin, New Mexico. In: Hinze, W.J. (ed.), The utility of regional gravity and magnetic anomaly maps. Tulsa, Oklahoma, *Soc. Expl. Geophy.*, p.181-197.
- Courtillot V., 1982. Propagating rifts and continental breakup. *Tectonics*, Vol.1,p.239-256.
- Dewey F.J., Pitman C.W., Ryan F.B.W., Bonnin J., 1973. Plate tectonics and the evolution of the Alpine system. *Bull. Geol. Soc. Amer.*, v.84, p.3137-3180.
- Dewey J.F., Booth J.E., Faux F.A., Johnson W.R., Kenzie J.K., McDowell E.H., El Ghoul A., 1989. Tectonic and Basin Evolution of the Libyan Offshore Region in its Central Mediterranean Tectonic Setting. *Internal report prepared under contract for Sirte Oil Company*, Brega, Libya, 254p.
- Di Paola G.M. 1973. The Island of Linosa (Sicily channel). *Bull. Volcan.*, Vol. 37, p.149-174.
- Finetti I., 1982. Structure, stratigraphy and evolution of central Mediterranean. *Boll. Geof. Teor. Appl.*, Vol.24, p.247-312.
- Finetti I., 1984. Geophysical study of the Sicily Channel rift zone, *Boll. Geof. Teor. Appl.*,Vol.26,p.1-28.
- Finetti I., 1985. Structure and evolution of the central Mediterranean (Pelagian and Ionian Seas), In: Geological evolution of the Mediterranean basin; D.J. Stanley and F.C. Wezel (eds.), Springer-Verlag, p.215-230.
- Jongsma D., Van Hinte J.E., Woodside J.M., 1985. Geologic structure and neotectonics of the North Africa Continental Margin south of Sicily. *Marine and petroleum Geology*, vol.2, p.156-179.
- Kearey P., 1991. A Possible Source of the South-Central England Magnetic anomaly: basaltic rocks beneath the London Platform. *Journal of the Geological Society of London*, v 148, p.775-780.
- Livermore R.A., Simth A.G., 1985. Some boundary conditions for the evolution of the Mediterranean Region. In D.J. Stanley and F.C.Wezel (Editors) *Geological Evolution of the Mediterranean Basin*: Springer-Verlag, New York, p. 83-98.

- Millingan P.R., Gunn P.J. 1997. Enhancements and presentation of airborne geophysical data. ASGO Journal of Australian Geology and Geophysics, 17(2), 31-38.
- Parnell J. 1985. Hydrocarbon source rocks, reservoir rocks and migration in the Orcadian Basin. *Scott. J. Geol.*, Vol.21, p.321-336.
- Pavoni N., 1993. Pattern of mantle convection and Pangaea break-up, as revealed by the evolution of the African plate. *J. Geol. Soc. London*, Vol.150, p.953-964
- Pitman W.C., Cochran J.R., Ryan W.B.F., Ladd J.W., 1981. Evolution of the Libyan margin, Annex II-6, A study of the Libyan Tunisian continental shelf, p.1-12.
- Reid A. B., Allsop J. M., Granser H., Millet A. J., Somerton I. W., 1990. Magnetic interpretation in three dimensions using Euler deconvolution. *Geophysics*. 55(1), 80-91.
- Seddig H. M., 1992. Sedimentology and basin analysis: part of NW Libyan offshore. *PhD Thesis*, University of Wales, 272p.
- Smith B., Derder M.E.M., Henry B., Bayou B., Amenna M., Djellit H., Yelles A.K., Garces M., Beamud E., Callot J.P., Eschard R., Chambers A., Aïfa T., Aït Ouali R., Gandriche H., 2006. Relative importance of the Hercynian and post-Jurassic tectonic phases in the Saharan platform: a Paleomagnetic study of Jurassic sills in the Reggane basin (Algeria). *Geophys. J. Int.*, 167, p.380-396, doi: 10.1111/j.1365-246X.2006.03105.x
- Spector A., Grant F.S., 1970. Statistical Models for Interpreting Aeromagnetic data. *Geophysics*, v 35, p. 293-302.
- White N., 1987. Nature of Lithospheric Extension in the North Sea. *Geology*, v 17, p. 111-114.
- White R., McKenzie D., 1989. Magmatism at rift zones: The generation of volcanic continental margins and flood basalts. *Journal of Geophysical Research*, Vol.94, p. 7685-7722.
- Winkler H.G., 1979. Petrogenesis of metamorphic rocks, *Springer-Verlag*, Berlin, 348p.
- Zarudski E.F.K, 1972. The Strait of Sicily a geophysical study, *Revue de Géographie physique et de Géologie dynamique*, Vol.14, p.11-28.
- Ziegler P.A., 1992. Plate Tectonics, Plate Moving Mechanisms and Rifting. *Tectonophysics*, v 215, p.9-34.

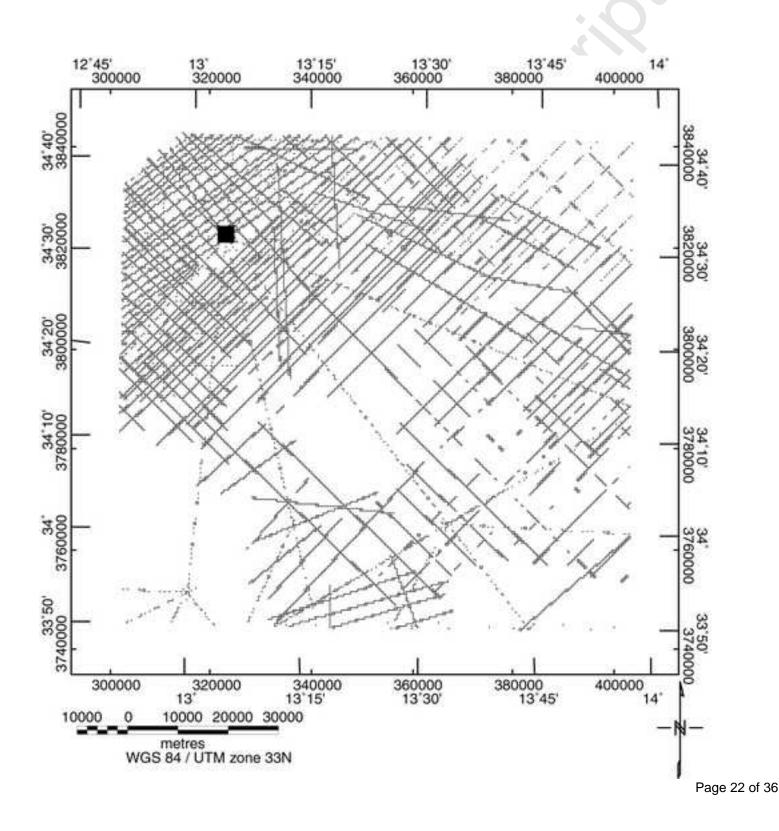
Figure captions

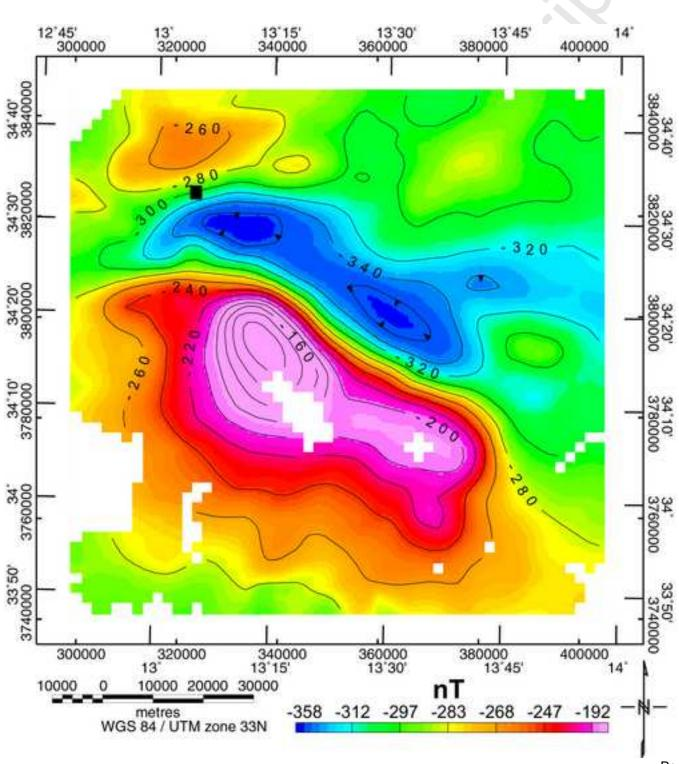
- **Figure 1.** Tectonic and morphologic elements of the Pelagian area offshore Libya (modified after Dewey, 1989).
- **Figure 2.** Location of magnetic and gravity survey from ship-borne profiles, run during the seismic survey, within the study area in the period 1975-1987. Black square: Jarrafa-1 borehole.
- **Figure 3.** Jarrafa magnetic (a) and gravity (b) anomaly maps with respective contour intervals of 20 nT and 1 mGal.
- **Figure 4.** Lithology of the Jarrafa-1 borehole. 1: level of *Globigerina*, 2: Glauconite, 3: Marls, 4: Clays, 5: Chalk, 6: Limestones, 7: Basalts, 8: Volcanic breccias, 9: Bioclastics, 10: Bivalves, GR: Gamma Ray log (API unit), ΔT: Sonic log (μs/ft), D: depth (m).
- **Figure 5. a-** Power spectrum of the Jarrafa magnetic anomaly. It shows three slopes namely 1, 2, 3 respectively at 2.7 km, 5.0 km and 11.0 km depth corresponding to three levels of magnetization. **b-** Power spectrum of the Jarrafa gravity anomaly showing roughly the same slopes (1-3) at similar depths (2.3 km, 5.0 km and 9.4 km) except (4) for the deepest source (13.0 km), probably corresponding to the base of the causative body.
- **Figure 6. a-** Comparison of Bouguer gravity map with pseudogravity field (contours) for induced magnetization at the present day field (D=0°, I=47°). Line contour interval: 1 mGal. **b-** Comparison of Bouguer gravity map with pseudogravity field (contours) for the total magnetization of D=-16°, I=23° and a ratio of density contrast to intensity of magnetization of unity. Line contour interval: 1 mGal.
- **Figure 7. a-** Three-dimensional model of the Jarrafa magnetic anomaly, represented by contours on the centres of the tops of the prisms. Contour interval: 1 km. **b-** Calculated magnetic anomaly of the 3D model of figure 7a, based on the magnetization effect of each given prism. Contour interval: 20 nT.
- **Figure 8. a-** Three-dimensional model of the Jarrafa gravity anomaly represented by contours on the centres of the tops of the prisms. Contour interval: 1 km. **b-**

- Computed gravity anomaly of the 3D model of figure 8a, based on the density contrast effect of each given prism. Contour interval: 1 mGal.
- **Figure 9. a-** Location of the maxima (x) of total horizontal gradient of the pseudogravity field (mGal/m). **b-** Total horizontal gradient of the gravity data with the location of the maxima (x).
- **Figure 10.** Euler solutions for depth estimates (2-10 km). RTP is shown by contours (contour intervals: 10 nT (50 nT) for thin (thick) line). The coloured circle indicates the depth to the magnetic source and the centre of the circle indicates the position of the source.
- **Figure 11.** Structural interpretation derived from magnetic and gravity data. Notice that a sinistral strike-slip (arrows) occurred after the structuration of the Jarrafa basin.

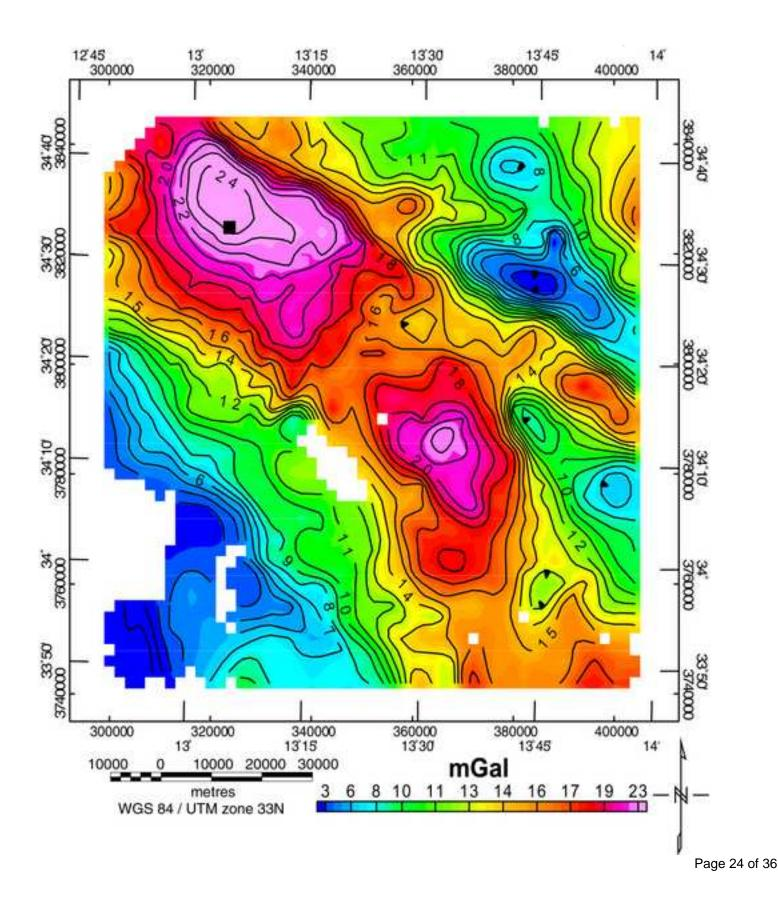


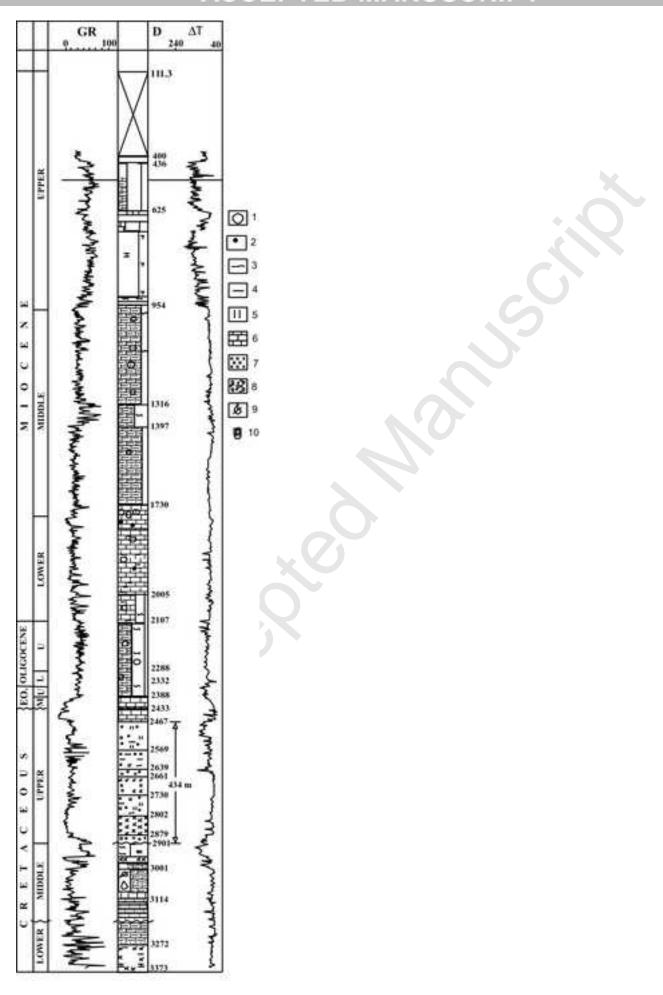
Page 21 of 36

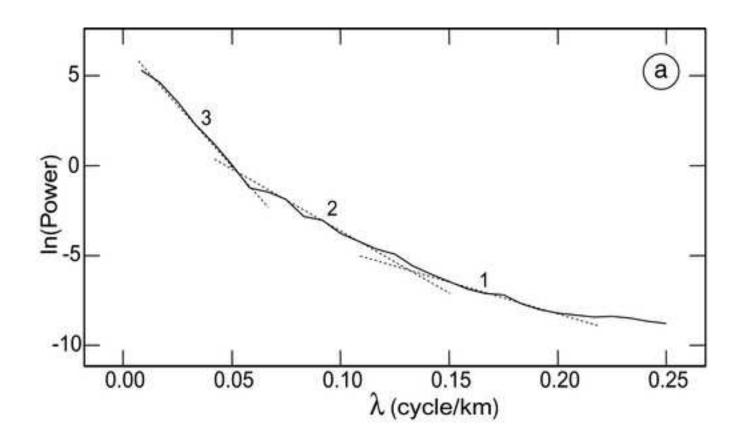


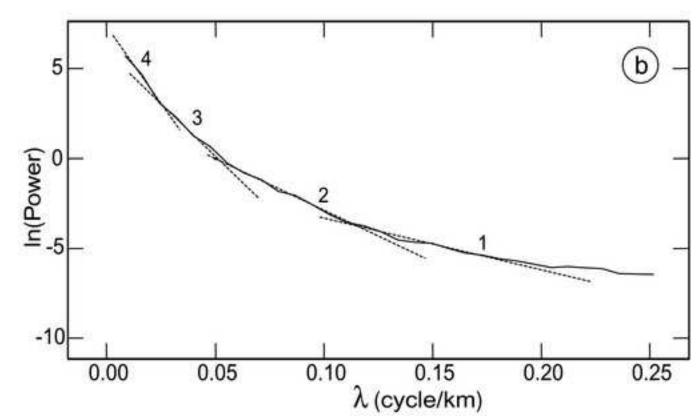


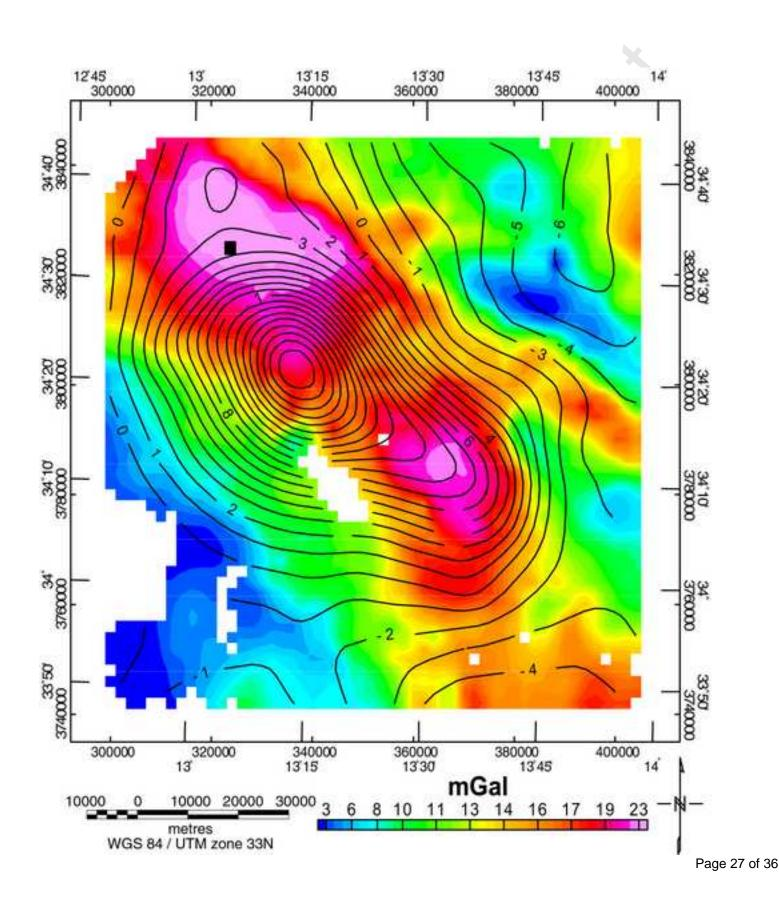
Page 23 of 36

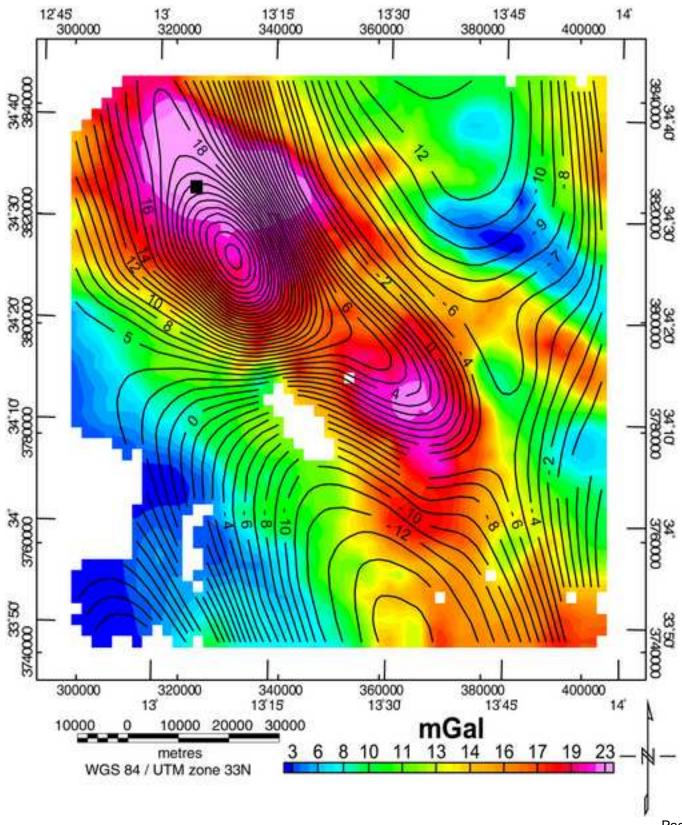


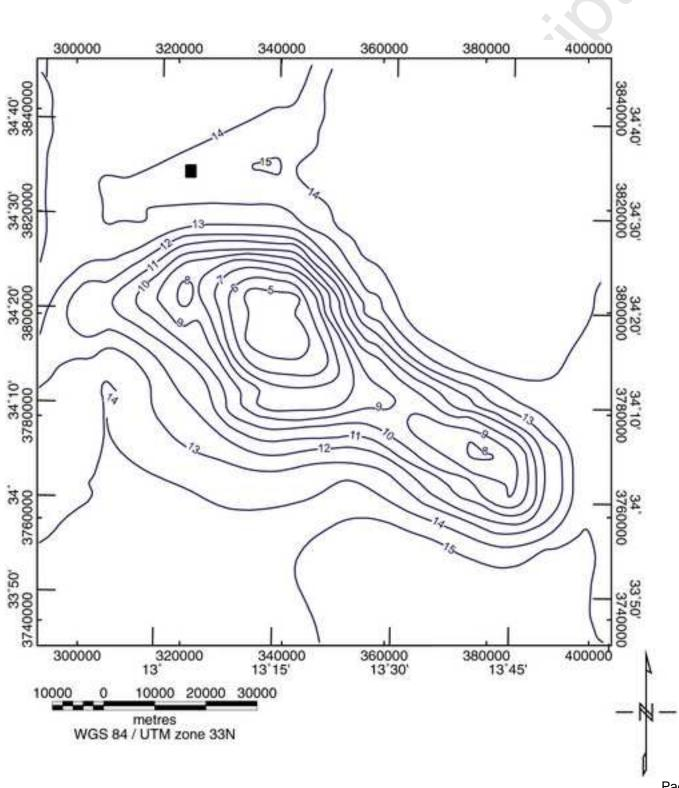


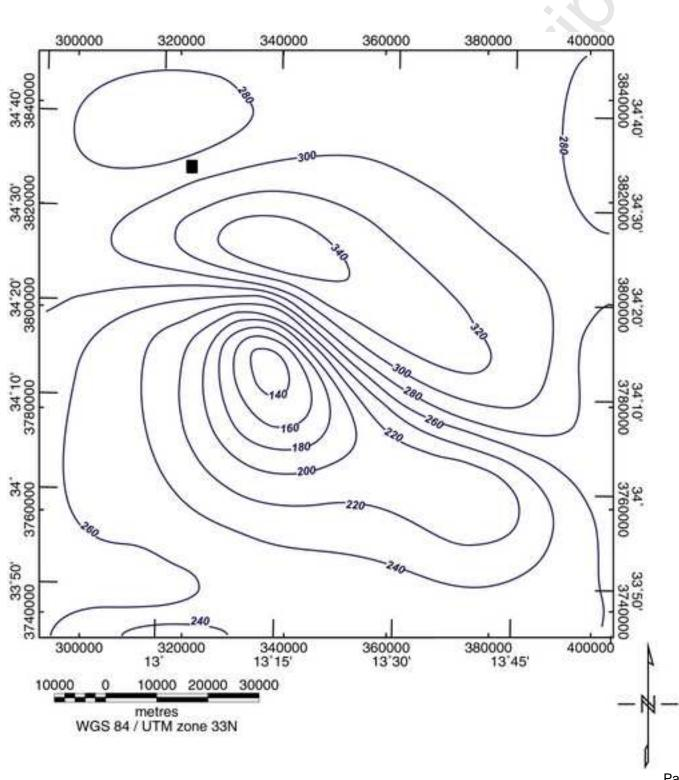


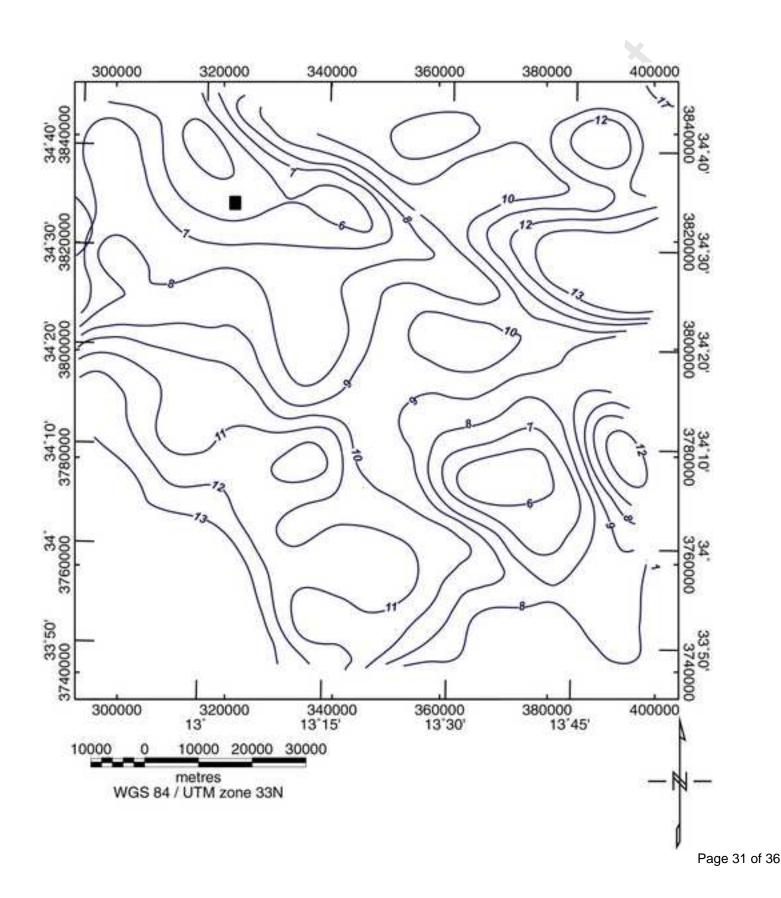


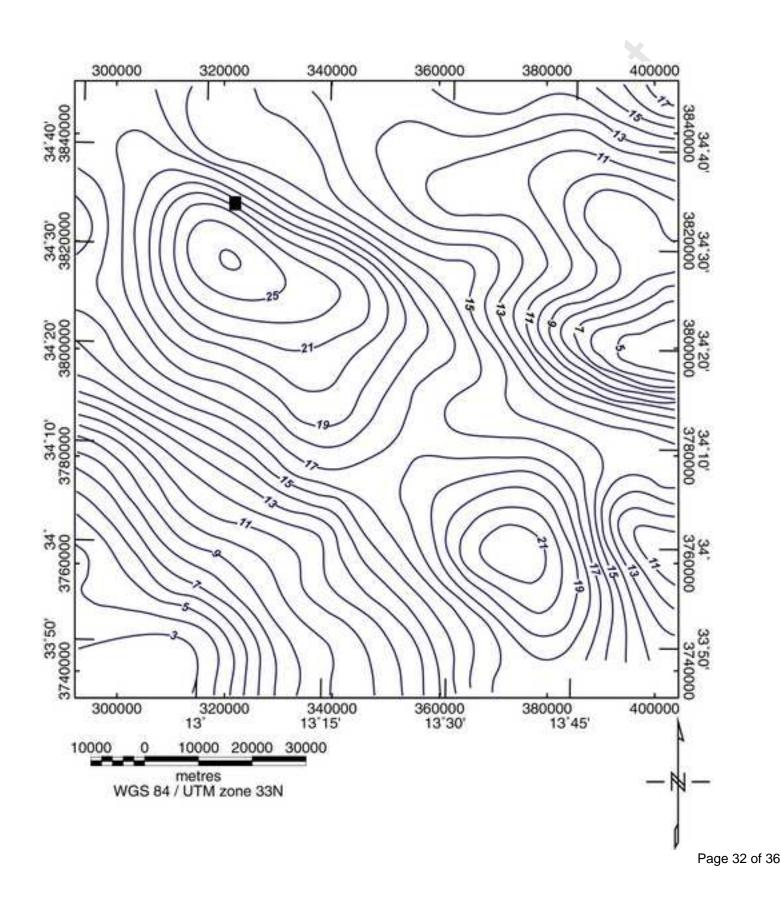


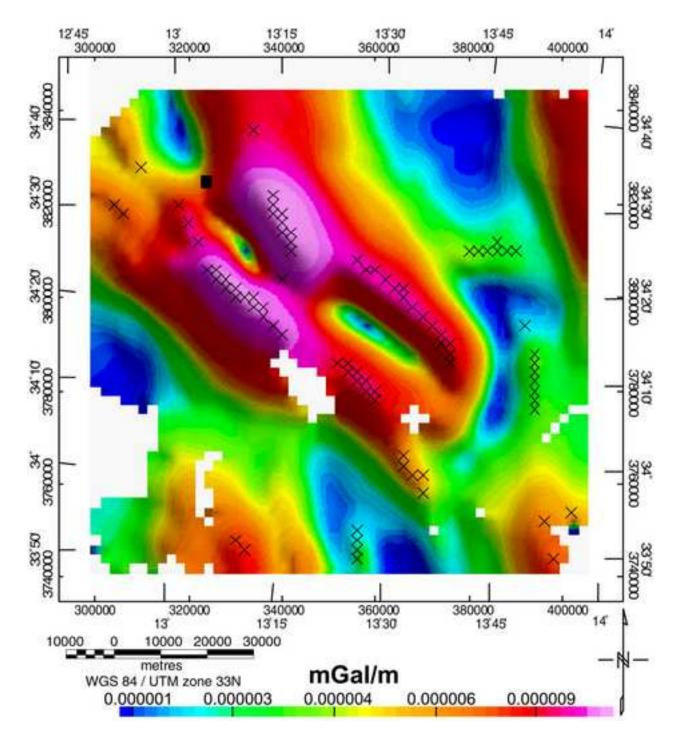


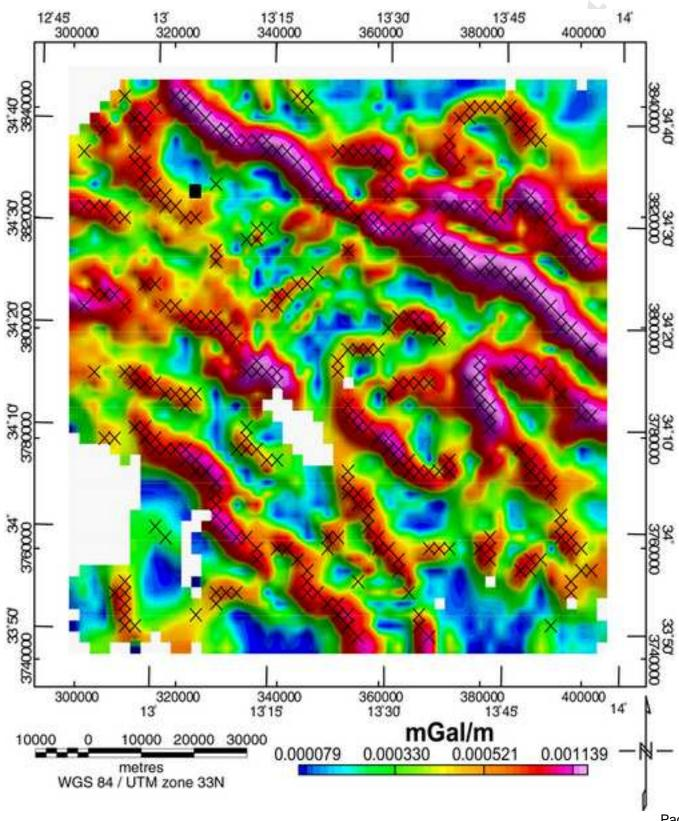


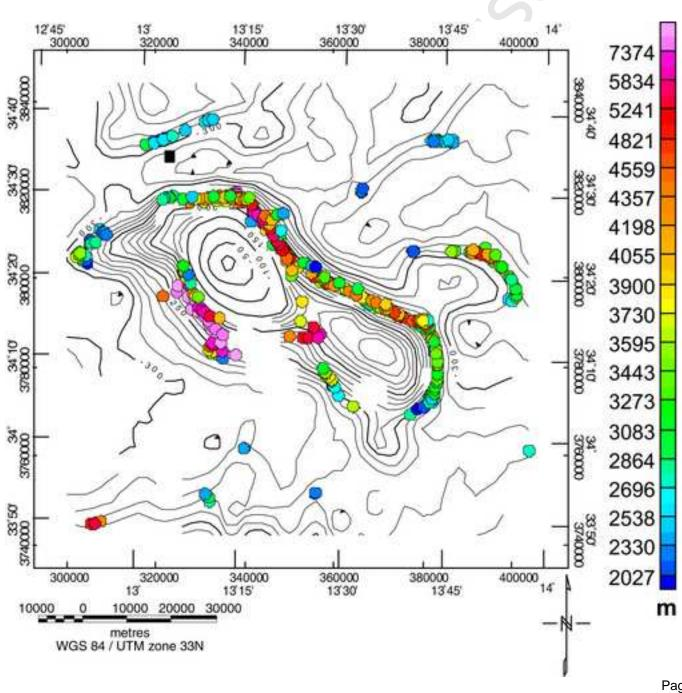












Page 35 of 36

